J Mater Sci (2007) 42:7109–7115
DOI 10.1007/s10853-007-1556-3

# Electrical properties and positron annihilation study of $(Ba_{1-x}Ho_x)TiO_3$ ceramics

**Fanggao Chang · Tao Li · Yongxia Ge · Zhenping Chen · Zhongshi Liu · Xiping Jing**

Received: 2 November 2006 / Accepted: 26 January 2007 / Published online: 5 May 2007


**Abstract** DC resistivity, dielectric constant, dielectric loss and positron annihilation spectra of $(Ba_{1-x}Ho_x)TiO_3$ ceramics have been measured as a function of holmium concentration $x$. It has been found that the DC resistivity of $(Ba_{1-x}Ho_x)TiO_3$ is strongly dependent on the Ho content: it decreases three orders of magnitude and reaches a minimum at $x = 0.4\%$. Doping with 0.6% holmium increases the permittivity of $BaTiO_3$ by approximately three times (from ~1,300 to ~4,000), with only a slight increase in the corresponding dielectric loss. The local electron density and defect concentration estimated using positron annihilation technique conforms well to the features found in the dielectric and resistivity measurements. The results have been discussed in terms of a mixed compensation model.

## Introduction

$BaTiO_3$ is an important ferroelectric material with many industrial applications, such as capacitors, positive temperature coefficient of resistivity (PTCR) thermistors, piezoelectric devices, optoelectronic elements etc. Many theoretical and experimental studies aimed at preparing techniques, modeling and characterizing have been carried out [1–4]. However some of the properties of pure $BaTiO_3$, such as small permittivity, large dissipation factor, limit its usefulness in certain areas. To improve the dielectric behavior of $BaTiO_3$, it is often doped with trivalent-elements [5–7]. It has been found that trivalent-element-doped $BaTiO_3$ ceramics show much better dielectric properties with a significant increase of permittivity, as well as an interesting dielectric relaxation behavior [8]. However, the dielectric properties and defect structure of $BaTiO_3$ ceramics doped with trivalent element Ho, to our knowledge, have not been investigated.

Positron lifetime is very sensitive to structural defects in solids. Therefore, positron annihilation technique has been widely used as an efficient probe of defect structure in solids [9]. For example, it has been applied to characterize GaAs [10], as well as the oxygen vacancies in high-temperature superconducting ceramics [11]. In this paper, the positron annihilation, as well as the X-ray diffraction technique, is used to investigate the effects of trivalent element Ho doping on the crystal structure and dielectric properties of $BaTiO_3$ ceramics.

## Experimental procedure

$(Ba_{1-x}Ho_x)TiO_3$ ceramics with $x = 0$, 0.2, 0.4, 0.6, 0.8, 1.0, 1.2% were prepared using raw materials of $BaCO_3$, $TiO_2$ (>99%) and $Ho_2O_3$ (>99.99%). The powders were mixed and milled with alcohol followed by calcinations at 1,150 °C for 3 h. The resulting powders were then granulated by adding polyvinyl alcohol. The powders were subsequently dried, milled and pressed with a pressure of 100 MPa into pellets of 13 mm in diameter and 1 mm in thickness. Finally the pellets were sintered at 1,350 °C for 2.5 h. The relative density of the samples are 92.42, 92.83,

F. Chang (✉) · Y. Ge
College of Physics and Information Engineering, Henan Normal University, Xinxiang 453007, P.R. China
e-mail: chfg@henannu.edu.cn

T. Li · Z. Chen
Department of Technology and Physics, Zhengzhou University of Light Industry, Zhengzhou 450002, P.R. China

Z. Liu · X. Jing
College of Chemistry & Molecular Engineering, Peking University, Beijing 100871, P.R. China

93.41, 94.03, 94.69, 95.38, 96.11% for corresponding Ho contents, respectively (the theoretical density of pure $BaTiO_3$ is 6.02 g/cm$^3$ [12]), which can be ascribed to the substitution of heavier holmium ions for much lighter barium ions. X-ray diffraction using CuK$\alpha$ radiation was carried out to determine the crystallographic structure. The dielectric constants and dissipation factor of the samples at room temperature 25 °C were measured using an Agilent 4294A Precision Impedance Analyzer at frequencies of 1 kHz, 10 kHz and 1 MHz, respectively.

The positron annihilation lifetime spectra of the samples were measured at room temperature (20 ± 0.5 °C) using an American ORTEC-100U fast–fast coincidence lifetime spectrometer. A $^{22}$Na positron source with activity 0.37 MBq, deposited on a thin Mylar film, was sandwiched together with two identical sample pieces. Each spectrum contains more than $10^6$ counts. Taking into account the background and source contributions, the lifetime spectra were analyzed in two positron lifetime components using the POSTRONFIT-EXTENDED program.

## Results and discussion

### X-ray diffraction analysis

Figure 1 shows the X-ray diffraction patterns of three Ho-doped $BaTiO_3$ samples. The crystal structure of $(Ba_{1-x}Ho_x)TiO_3$ is similar to that of pure $BaTiO_3$: the overall tetragonal lattice structure has not been affected by Ho-doping up to $x = 1.2\%$. Substitution of smaller Ho ions for large Ba ions should decrease the size of some unit cells and we would expect the diffraction peaks shift towards high 2-theta values with increasing Ho content. However, Fig. 1 shows just the opposite: the diffraction peaks shift slightly to the low 2-theta end as the Holmium concentration increases. The physical origin of this anomalous shift is not clear. One possibility is that there may exist a secondary phase accompanying the holmium doping, similar to the situation associated with Sm-doped $BaTiO_3$ ceramics [13].

### The effect of holmium doping on the DC resistivity of $BaTiO_3$ ceramics

Figure 2 shows the DC resistivity of Ho-doped $BaTiO_3$ samples as a function of holmium content $x$. The resistivity is strongly dependent on the dopant content. It decreases sharply with increasing dopant content for $x \leq 0.4\%$, reaching a minimum at a dopant content level of $x = 0.4\%$, and then increases for $x \geq 0.4\%$. The difference between the resistivity of pure $BaTiO_3$ and the minimum at $x = 0.4\%$ is about three orders of magnitude. The U-shaped curve found here is similar to that observed in the Sm-doped $BaTiO_3$ ceramics [13] and can be understand in terms of a mixed compensation model.

During the sintering processing, trivalent element Ho acts as a donor dopant replacing Ba in the $BaTiO_3$ perovskite lattice:

$$2Ho_2O_3 + 4TiO_2 \rightarrow 4Ho^{\cdot}_{Ba} + 4(Ti^{4+\cdot}e) + 12O^{2-} + O_2 \quad (1)$$

$$2Ho_2O_3 + 6TiO_2 \rightarrow 4Ho^{\cdot}_{Ba} + 6Ti^{4+} + 18O^{2-} + 2V''_{Ba} \quad (2)$$

where $Ho^{\cdot}_{Ba}$ is the dopant on a Ba-site and $V_{Ba}''$ a barium cation vacancy in the $BaTiO_3$ perovskite lattice.

The trivalent element Ho located at Ba sites carries excess negative charge (electron), which for maintenance of electric neutrality, can be compensated in two different ways. First, when the dopant content is less than a certain value ($x = 0.4\%$ in our case), the doping behaves as an electron-compensator. The concentration of excess electrons will then equal that of the donor ions. The excess

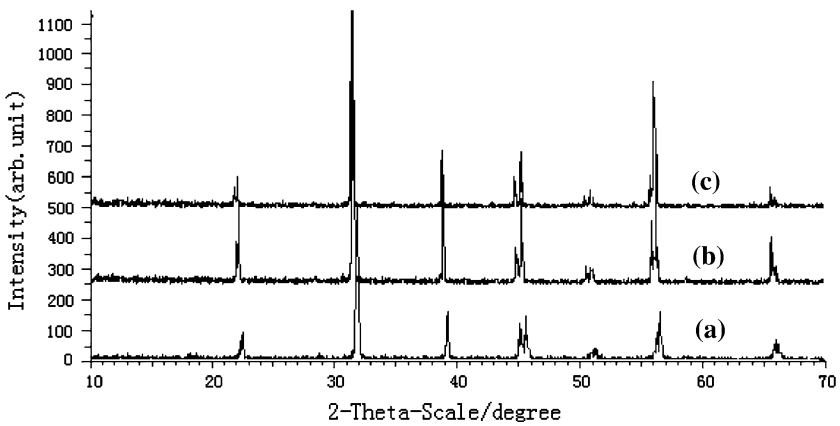


**Fig. 1** X-ray diffraction spectra of $(Ba_{1-x}Ho_x)TiO_3$ ceramic samples (a:$x = 0$, b:$x = 0.6\%$, c:$x = 1.2\%$)

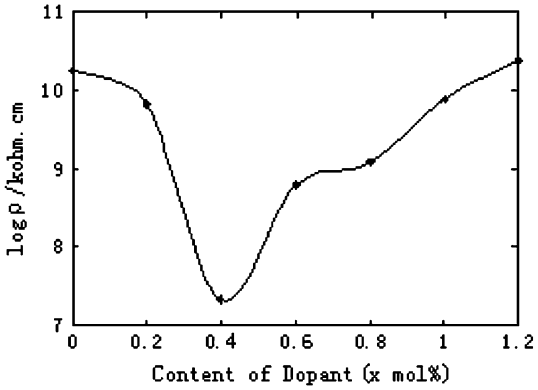


**Fig. 2** DC resistivity of $(Ba_{1-x}Ho_x)TiO_3$ ceramic samples versus Ho content $x$

electrons are weakly bonded by $Ti^{4+}$, forming quasi-free electrons that will consequently increase the conductivity of the material. Second, cation vacancy-compensation becomes gradually dominant when the dopant content is higher than the critical value. As a result, Ba vacancies will be formed as indicated by Eq. 2.

Therefore, it is reasonable to assume that the DC resistivity behavior of the samples arises mainly from the coexistence of these two compensation processes at relatively low dopant content. This accounts for why low resistivity $BaTiO_3$ ceramics cannot be obtained by donor doping only [14]. When the dopant content is lower ($x \leq 0.4\%$), the electron-compensation is predominant and the local electron density becomes higher, the resistivity decreasing accordingly. As the dopant content is increased ($x \geq 0.4\%$), the Ba vacancies become predominant. The number of structural defects in the material increases rapidly, resulting in a sharp increase in the resistivity. The effect of donor-introduced electrons on the resistivity can be neglected at high doping level, compared with that of vacancy-compensation.

## The effect of holmium doping on the dielectric properties of $BaTiO_3$ ceramics

Figure 3 shows the relative dielectric constant $\varepsilon_r$ and dielectric dissipation factor tan$\delta$ of $BaTiO_3$ ceramics doped with various Ho contents, measured at selected frequencies. It can be seen that $\varepsilon_r$ and tan$\delta$ reach maximum values at approximately $x = 0.6\%$ and $x = 0.4\%$, respectively. Doping with 0.6% Ho increases the dielectric constant from a value of ~1,300 to the maximum value ~4,000, approximately three times as large as that of pure $BaTiO_3$. While only a slight increase in the corresponding dielectric dissipation factor is observed. In addition, the dielectric constant $\varepsilon_r$ decreases with increasing frequency, due to a dielectric relaxation process. The dielectric dissipation factor tan$\delta$

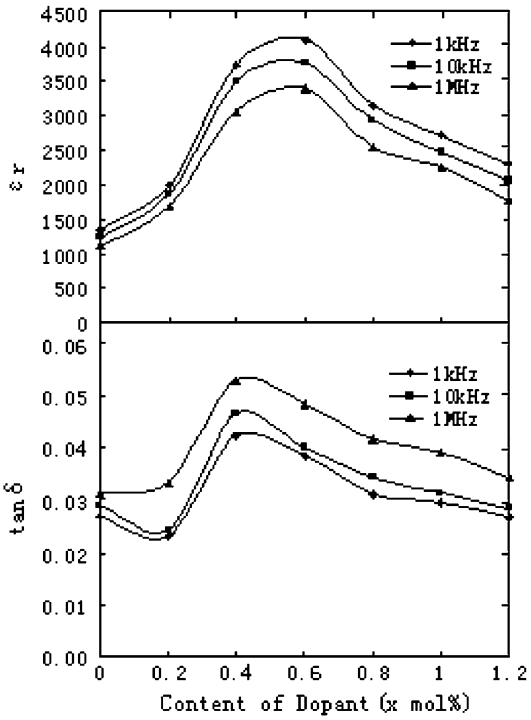


**Fig. 3** Dielectric constant and dissipation factor of $(Ba_{1-x}Ho_x)TiO_3$ versus Ho content $x$ measured at 1 kHz, 10 kHz and1 MHz

however, increases with operating frequency, which is consistent with the normal dielectric loss behavior.

According to the previous discussion on the mixed-compensation mechanism, quasi-free electrons and vacancies coexist in the doped samples. It was reported that the barium (strontium) vacancies are initially formed at the grain boundary and diffuse gradually into the grains of $BaTiO_3(SrTiO_3)$ [15]. The electrons and barium vacancies are inhomogeneously distributed within the grains and at the grain boundaries. The two types of compensation (electron and vacancy) result in space-charge polarization, which contributes to the dielectric constant. For Ho contents of $0 \leq x \leq 0.4\%$, the quasi-free electron concentration is proportional to $x$. Applying an electrical field would drive these weakly bonded quasi-free electrons to hop a distance from the positive dopant ions to form dipole moments. Obviously, dielectric constant would increase with the number of electrons introduced by holmium doping. The higher the electron-concentration, the higher the dissipation factor caused by electrical conduction [14]. The increase of dielectric constant and dielectric dissipation factor with doping concentration less than 0.4% may thus be attributed to the polarization associated with the quasi-free electrons introduced by holmium doping. The maximum value of tan$\delta$ at $x = 0.4\%$, the point at which the local quasi-free electron density reaches the maximum, agrees well with the minimum resistivity shown in Fig. 2.

As the dopant content increases further above $x = 0.4\%$, the mechanism of vacancy-compensation begins to emerge rapidly. The number of Ba vacancies increases relative to the number of quasi electrons. Consequently the dielectric dissipation factor becomes smaller with increasing doping concentration due to a decrease in the conductivity. However, the dielectric constant continues to increase until the dopant content reaches 0.6%, where a broad maximum is observed (Fig. 3). This may be ascribed to the space-charge polarization caused by the Ba-vacancies. Moreover, the mobility of the quasi-free electrons is reduced by the existence of defects related with the Ba-vacancies. As a result, the conductivity and subsequently the dissipation factor, as well as the dielectric constant decrease at high doping contents. The dielectric properties of these ceramic samples are mainly determined by the weakly bonded quasi-free electron density and the effects of space-charge polarization of Ba-vacancies is less important.

There have been a number of reports of permittivity being raised by introducing an increase in the internal electrical conductivity of dielectric materials [16–20]. Based on the results of computer simulation and an experiment in which water was added to lead zirconate titanate ceramic, Almond et al. [16, 17] demonstrated that large networks of randomly positioned resistors and capacitors exhibit electrical properties that are identical with the universal anomalous characteristics of many dielectric materials. It was shown that introducing a conducting phase into a ferroelectric material would result in a significant enhancement in permittivity with a power-law frequency dependence. Our results on holmium doped $BaTiO_3$ ceramics are in excellent agreement with the work presented in Ref. [16]. Trivalent doping increases the conductivity of the $BaTiO_3$ ceramic samples, leading to an increase in the dielectric constant that decreases with increasing frequency. This suggests that, at a microstructural level, $BaTiO_3$ ceramics behave as a network of conducting and capacitive regions and their dielectric properties could be described by the network of randomly positioned resistors and capacitors. It is noteworthy that the high permittivity raised by trivalent doping as well as by adding conductive phase to a dielectric material is an ''intrinsic'' bulk effect, not an ''extrinsic'' effect associated with grain boundaries suggested for the origin of the high permittivity in $CaCu_3Ti_4O_{12}$ and $(La_{0.4}Ba_{0.4}Ca_{0.2})(Mn_{0.4}Ti_{0.6})O_3$ ceramics in Refs. [18–20].

## Positron annihilation study of defect structure

In this work, the so-called two-state trapping model is adopted. Two positron lifetime components $\tau_1$ and $\tau_2$ have been resolved from the lifetime spectra. Theoretically, short lifetime $\tau_1$ and long lifetime $\tau_2$ correspond to the defect-free-annihilation lifetime $\tau_f$ and the defect-annihilation lifetime $\tau_d$, respectively. $I_1$ and $I_2$ are the intensities of short lifetime and long lifetime, respectively. In reality, due to the statistical nature of the fitting method, $\tau_1$ almost always include contributions from shallow-trap annihilation and have a larger value than could be expected from the defect-free-annihilation lifetime.

The positron lifetime parameters are shown in Fig. 4. The short lifetime $\tau_1$ decreases from ~231 ps for the pure $BaTiO_3$ to ~221 ps for a sample with Ho content of 0.4%. The corresponding intensity $I_1$ increases slightly with Ho doping and reaches a maximum at $x = 0.4\%$. These

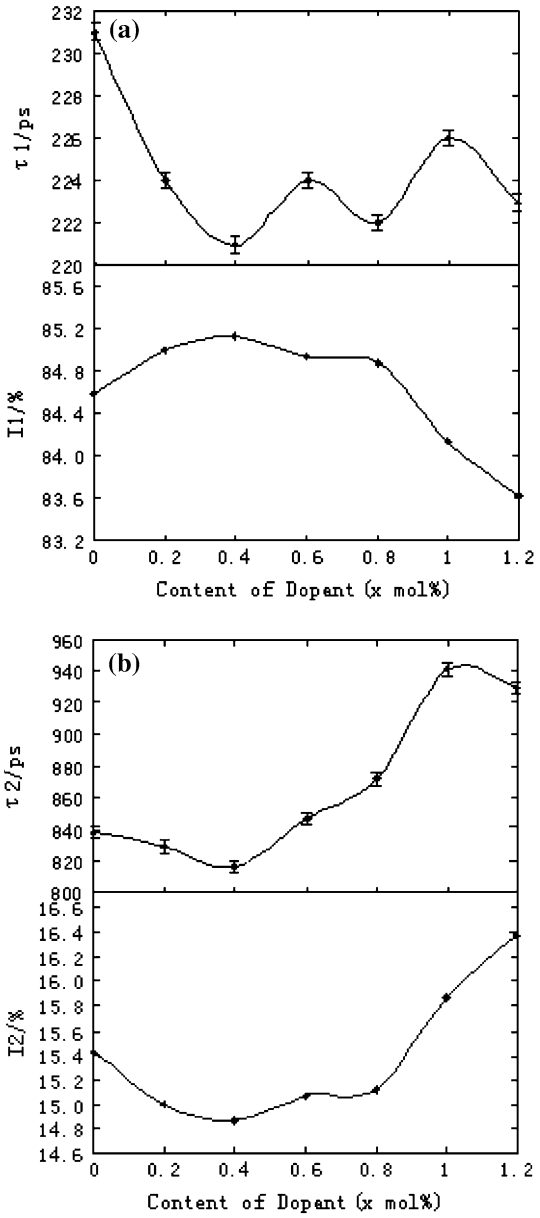


**Fig. 4** Positron lifetime parameter $\tau_1$, $I_1$ (**a**) and $\tau_2$, $I_2$ (**b**) as a function of dopant content $x$ for $(Ba_{1-x}Ho_x)TiO_3$ samples

observations agree well with the results of resistivity and dielectric measurements given in Figs. 2 and 3. The variation of $\tau_1$ and $I_1$ is a direct consequence of the change in local electron density. As mentioned above, the local electron density reaches a maximum at a doping level 0.4%. It is this increase in local electron density that results in the minimum $\tau_1$ and maximum $I_1$ in Fig. 4a.

The long lifetime $\tau_2$ decreases slightly with increasing Ho content as $x < 0.4\%$ and increases rapidly afterwards (Fig. 4b). The corresponding intensity $I_2$ varies similarly. In general, long lifetime annihilation may be caused by structural defects such as vacancies, vacancy clusters, and grain boundary etc. The variation of $I_2$ corresponds to the change of vacancy density if the defect densities are not too high and not all the positrons become trapped. Conversely, if the defect concentration is large enough, positron trapping will be saturated and the intensity $I_2$ is not any more sensitive to the defect concentration but reflects changing trapping fractions for different defects and changing open volume. When dopant level is small, the number of Ba vacancies is also small and almost independent of doping content. As the Ho doping content exceeds 0.4%, the number of Ba vacancies increases rapidly and some of them may form larger vacancy clusters or even microvoids. This accounts for the large $\tau_2$ at high doping level (>0.4%). The rapid increase of $I_2$ at high doping level observed in Fig. 4b is consistent with an increase in Ba vacancy density evidenced by resistivity and dielectric measurements and suggests that the defect concentration at this doping level has not been saturated.

It should be noted that the long lifetime component determined here seem to be too large to be attributed to the annihilation at normal vacancies. Theoretical calculation gave lifetime values of 162 ps for oxygen vacancy and 293 ps for Ba vacancy [21]. For large vacancy clusters the saturation lifetime could be as high as 500 ps. A lifetime close to 1 ns may be an indication of annihilation of positronium in the sample. From the discussion presented above, it is reasonable to assume that positroniums have been formed at Ba vacancy clusters or grain boundaries in these samples. Furthermore, the values of $\tau_1$ and $\tau_2$ of undoped $BaTiO_3$ obtained in this work are much higher than some of the experimental values found before [22]. One possible reason for the discrepancy may be that polycrystalline ceramic samples with different microstructure were used. Depending on the size of grains, density of pores and density of positron traps inside the powder-particles or grains of the ceramic sample, positron lifetime could be ~300 ps when annihilated at grain boundaries, or even as high as ~600 ps if trapped at inner surfaces or interfaces [23]. Therefore careful consideration needs to be taken when compare positron annihilation data obtained from samples prepared in different laboratories and using different techniques. Hopefully this effect would not matter too much in our case, as all the samples were prepared using the same method and only relative changes of annihilation parameters versus dopant content are our main concern.

To estimate the local electron density and the defect concentration in the ceramics, we need to calculate the average positron lifetime and bulk lifetime. The bulk lifetime $\tau_b$ and the average lifetime $\bar{\tau}$ can be found from the lifetime and the intensity of the two components by the following equations [24]:

$$\tau_b = \frac{1}{\lambda_b} = \frac{1}{I_1/\tau_1 + I_2/\tau_2} \tag{3}$$

$$\bar{\tau} = I_1\tau_1 + I_2\tau_2 \tag{4}$$

The calculated values of $\tau_b$ and $\bar{\tau}$ are plotted in Fig. 5. It is known that $\tau_b$ and $\bar{\tau}$ is associated with the bulk characteristics of the materials and the feature of defects, respectively. According to Eq. 3, the bulk lifetime is determined mainly by the short lifetime component and the contribution from long lifetime components is relatively small. The rapid decrease in $\tau_b$ at low Ho contents results from an increase in the electron density of materials (upper curve in Fig. 5). The increase of $\tau_b$ at high dopant content indicates an increase in the number of Ba vacancies. The average lifetime $\bar{\tau}$ behaves similarly to bulk lifetime in

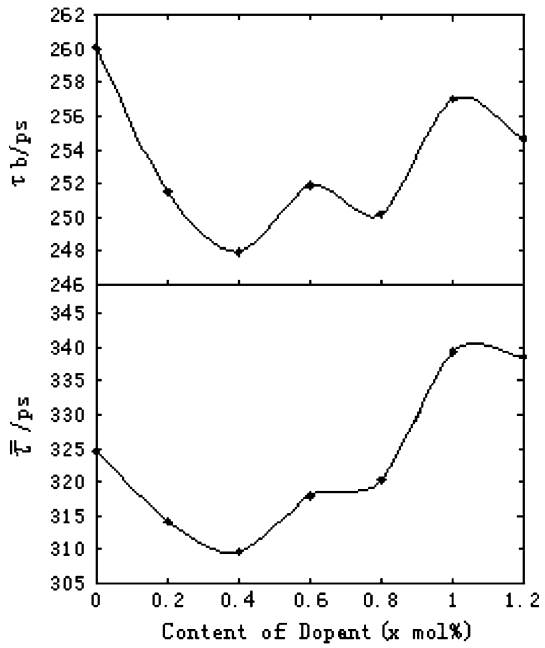


**Fig. 5** Bulk and average positron annihilation lifetimes as a function of dopant content $x$ for $(Ba_{1-x}Ho_x)TiO_3$ samples

terms of dopant dependency. Again, there is a minimum in the curve of $\bar{\tau}$ in the vicinity of $x = 0.4\%$.

Knowing the values of positron bulk lifetime $\tau_b$ and average lifetime $\bar{\tau}$, the electron density $n_e$ and the defect concentration $C_v$ are calculated using the following equations [25, 26].

$$n_e = \frac{1}{\pi r_0^2 \bar{\tau} c} \tag{5}$$

$$C_v = \frac{k_v}{v r_v^2} \tag{6}$$

where

$$k_v = \frac{I_2}{I_1}\left(\frac{1}{\tau_b} - \frac{1}{\tau_2} + k_{mv}\right) \tag{7}$$

$$k_{mv} = \frac{\tau_1/\tau_{bloch} - I_2\tau_1/\tau_2 - I_1}{\tau_{mv} - \tau_1} \tag{8}$$

($r_0$, classical radius of electron; C, the velocity of light; $k_v$, $k_{mv}$, positron trapping ratio of micro voids and single vacancy, respectively; $v$, average velocity of positron; $r_v$, radius of micro void; $\tau_{bloch}$ and $\tau_{mv}$, the annihilation lifetime in Bloch state and single vacancies, respectively.)

Taking $\tau_{bloch} = 190$ ps and $\tau_{mv} = 240$ ps as a rough estimation, the local electron density and defects concentration have been calculated from the positron annihilation data. Figure 6 shows the curves of $n_e$ and $C_v$ versus Ho content.

It is clear that there is an increase of electron density for $0 \le x \le 0.4\%$. Additionally, there is an obvious increase of vacancy concentration for $x > 0.4\%$, which conform well to the compensation mechanism we have discussed in the previous sections. It is striking to see that three independent measurements lead to essentially the same conclusion. Features found using electrical, dielectric and positron annihilation techniques are all correlated to a single mechanism.

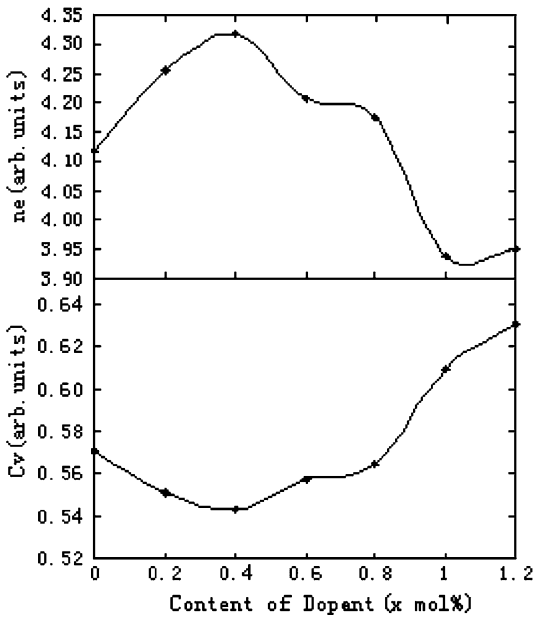


**Fig. 6** Electron density ($n_e$) and vacancy concentration ($C_v$) as a function of the dopant content $x$ for Ho-doped $BaTiO_3$ samples

## Conclusions

In summary, we have measured the electrical resistivity and dielectric constants of Ho-doped $BaTiO_3$ ceramics, as well as the positron annihilation lifetime in these materials. The following conclusions have been reached:

(1) The tetragonal lattice structure of $BaTiO_3$ has not been affected by Ho-doping up to 1.2%. However, a small shift of the X-ray diffraction peaks towards the low 2-theta end is observed with increasing holmium content, the physical origin of which is not yet clear.

(2) The resistivity of $(Ba_{1-x}Ho_x)TiO_3$ decreases with increasing dopant content for small $x$, and reaches a minimum at a dopant content level of $x = 0.4\%$. The minimum DC resistivity is three orders of magnitude smaller than that of pure $BaTiO_3$.

(3) Holmium doping can effectively increase the permittivity to a value of 4,000 that is three times as large as that for pure $BaTiO_3$ ceramics, while only a slight increase in the corresponding dielectric dissipation factor is observed. The permittivity $\varepsilon_r$ of $BaTiO_3$ ceramics decreases and the dissipation factor $\tan\delta$ increases with measurement frequency for all the Ho contents.

(4) The positron annihilation spectra and the local electron density and defect concentration obtained with the positron annihilation technique confirm the mixed compensation model evidenced by the features found in the dielectric and resistivity measurements.

**Acknowledgements** This work was supported by National Natural Science Foundation of China (Project No.: 60571063). The project was partially sponsored by the Scientific Research Foundation for the Returned Overseas Chinese Scholars, State Education Ministry.

## References

1. Lewis GV, Catlow CRA, Casselton J (1985) J Am Ceram Soc 68:555

2. Han JH, Kim DY (1998) Acta Mater 46:2021
3. Cho WS (1997) J Phys Chem Solids 59:659
4. Gotor FJ, Perez-Maqueda LA, Criado JM (2003) J Eur Ceram Soc 23:505
5. Wei JZ, Zhang LY, Yao XJ (1999) Am Ceram Soc 82:2551
6. Chen CY, Tuan WH (1999) J Mater Sci Lett 18:353
7. Shannigrahi SR, Choudhary RN et al (1999) J Mater Sci Lett 18:345
8. Skanavi GI, Ksendzov IM, Trigubenko VA et al (1958) Soc Phys-JETP 6:250
9. Brandt W, Grance RE (1967) J Phys Rev Lett 21:16
10. Krause R, Saarinen K, Hartojarvi P, Polity A et al (1990) Phys Rev Lett 65:3329
11. Tang C, Li BR, Chen A (1990) Phys Rev B 42:8087
12. Demartin M, Herard C, Carry C, Lemaitre J (1997) J Am Cerm Soc 80:1079
13. Li ZC, Zhang H et al (2005) Mater Sci Eng B 116:34
14. Yu Z, Chen A (1993) J Phys: Condens Matter 5:1877
15. Phillips WR (1976) Res Rep 31:526
16. Almond DP, Bowen CR, Rees DAS (2006) J Phys D: Appl Phys 39:1295
17. Almond DP, Bowen CR (2004) Phys Rev Lett 92:157601
18. Li M, Feteira A, Sinclair DC (2005) J Appl Phys 98:084101
19. Sinclair DC, Adams TB, Morrison FD, West AR (2002) Appl Phys Lett 80:2153
20. Adams TB, Sinclair DC, West AR (2002) Adv Mater 14:1321
21. Ghosh VJ, Nielsen B, Friessnegg T (2000) Phys Rev B 61:207
22. Massoud AM, Krause-Rehberg R, Langhammer HT, Gebauer J, Mohsen M (2001) Mater Sci Forum 363–365:144
23. Staab TEM, Krause-Rehberg R, Kieback B (1999) J Mater Sci 34:3833. DOI: 10.1023/A:1004666003732
24. Hor PH, Meng RL, Huang ZJ, Chu CW (1990) Phys Rev Lett 64:1593
25. Petresen K, Thrance N, Trumy G (1976) Appl Phys 10:85
26. Vehanan A, Hautojarvi P, Johansson J et al (1982) Phys Rev B 25:762